Development 134, 2007-2016 (2007) doi:10.1242/dev.000885

The FERM protein Epb4.1l5 is required for organization of the neural plate and for the epithelial-mesenchymal transition at the primitive streak of the mouse embryo

Jeffrey D. Lee[1], Nancy F. Silva-Gagliardi[2], Ulrich Tepass[3], C. Jane McGlade[2] and Kathryn V. Anderson[1,*]

During early mouse development, a single-layered epithelium is transformed into the three germ layers that are the basis of the embryonic body plan. Here we describe an ENU-induced mutation, *limulus* (*lulu*), which disrupts gastrulation and the organization of all three embryonic germ layers. Positional cloning and analysis of additional alleles show that *lulu* is a null allele of the FERM-domain gene erythrocyte protein band 4.1-like 5 (*Epb4.1l5*). During gastrulation, some cells in *lulu* mutants are trapped in the primitive streak at an intermediate stage of the epithelial-mesenchymal transition; as a result, the embryos have very little paraxial mesoderm. Epithelial layers of the later *lulu* embryo are also disrupted: definitive endoderm is specified but does not form a gut tube, and the neural plate is broad and forms ectopic folds rather than closing to make the neural tube. In contrast to zebrafish and *Drosophila*, in which orthologs of *Epb4.1l5* control the apical localization and activity of Crumbs proteins, mouse Crumbs proteins are localized normally to the apical surface of the *lulu* mutant epiblast and neural plate. However, the defects in both the *lulu* primitive streak and neural plate are associated with disruption of the normal organization of the actin cytoskeleton. We propose that mouse Lulu (Epb4.1l5) helps anchor the actin-myosin contractile machinery to the membrane to allow the dynamic rearrangements of epithelia that mediate embryonic morphogenesis.

KEY WORDS: FERM, Epithelial morphogenesis, EMT, Cytoskeleton, Gastrulation, Actin, Crumbs, Mouse

INTRODUCTION

Proteins of the FERM-domain family regulate epithelial organization by linking membrane-associated proteins to the actin cytoskeleton (Bretscher et al., 2002; Mangeat et al., 1999). The mouse genome encodes at least 50 FERM proteins, but the functions of only a few, including the actin-binding proteins ezrin (also known as Vil2 – Mouse Genome Informatics), radixin, moesin, Nf2 (also known as merlin) and the erythrocyte protein band 4.1, have been characterized (Bretscher et al., 2002; Mangeat et al., 1999). Of these proteins, only Nf2, the product of the *Nf2* tumor suppressor gene, has been shown to be required for early embryonic development; embryos that lack Nf2 die shortly after the onset of gastrulation due to defects in the epithelial organization of the extra-embryonic ectoderm (McClatchey et al., 1997). Here we identify Lulu (Epb4.1l5) as another FERM protein that is essential for mouse development, and show that it has central roles in early embryonic morphogenesis.

During early postimplantation development, the single-layered columnar epithelium of the mouse epiblast is transformed over the course of 2 days into a three-layered embryo with a well-defined body plan (Tam and Gad, 2004). Beginning at embryonic day (E)6.5, cells at the primitive streak undergo an epithelial-to-mesenchymal transition (EMT) to give rise to the mesodermal and endodermal germ layers. Once generated, each germ layer undergoes a characteristic set of morphological changes: the mesenchymal cells of the mesodermal layer migrate around the embryonic circumference, endodermal cells form an epithelium that folds to generate the gut tube, and cells of the neural epithelium bend and contract their apical surfaces to generate a closed neural tube.

In an N-ethyl N-nitrosourea (ENU)-mutagenesis screen for mutations that affect the morphology of the mid-gestation mouse embryo, we isolated a mutation that we named *limulus* (*lulu*) based on the flat, plate-like morphology of the mutant embryos (García-García et al., 2005). *lulu* embryos have defects in the morphogenesis of all three germ layers: very little paraxial mesoderm is specified, the endoderm fails to form the gut tube, and the neural plate has an irregular shape and does not generate a neural tube. Based on positional cloning, we find that *lulu* is a null allele of the gene encoding the mouse FERM-domain protein erythrocyte protein band 4.1-like 5 (Epb4.1l5); the allele is designated *Epb4.1l5^{lulu}* and we refer to the allele here as *lulu* (Epb4.1l5 has also been called YMO1) (Laprise et al., 2006).

Homologs of *Epb4.1l5* play roles in specific aspects of *Drosophila* and zebrafish development (Hoover and Bryant, 2002; Hsu et al., 2006; Jensen and Westerfield, 2004; Laprise et al., 2006). The *Drosophila* ortholog of *Epb4.1l5*, named *yurt*, is required for epithelial polarity and dorsal closure in the embryo, and for photoreceptor morphogenesis (Hoover and Bryant, 2002; Laprise et al., 2006). Yurt appears to act as a negative regulator of Crumbs, a key determinant of the apical domain of epithelial cells (Tepass et al., 1990; Wodarz et al., 1995). The zebrafish *epb41l5* (also known as *mosaic eyes*; *moe*) gene is required for the layering of the retina and inflation of the brain ventricles, and, like Yurt, regulates the size of the apical membrane domain, possibly also via the negative regulation of Crumbs (Hsu et al., 2006; Jensen et al., 2001; Jensen and Westerfield, 2004).

Analysis of the tissues affected in *lulu* mutant embryos reveals that Lulu has specific roles in the EMT at gastrulation and in the organization of the pseudo-stratified epithelium of the neural plate.

[1]Developmental Biology Program, Sloan-Kettering Institute, 1275 York Avenue, New York, NY 10021, USA. [2]The Hospital for Sick Children, Arthur and Sonia Labatt Brain Tumor Research Center and Department of Medical Biophysics, University of Toronto, Toronto, Ontario M5G 1X8, Canada. [3]Department of Cell and Systems Biology, University of Toronto, Toronto, Ontario M5S 3G5, Canada.

*Author for correspondence (e-mail: k-anderson@ski.mskcc.org)

Accepted 20 March 2007

In both contexts, the defects in tissue organization are associated with dramatic changes in the organization of the actin cytoskeleton. In contrast to the results in zebrafish and *Drosophila*, Crumbs localization appears not to be affected in *lulu* mutants. The results indicate that Lulu is crucial for the dynamic rearrangements of the actin cytoskeleton that occur during the morphogenesis of epithelial tissues.

MATERIALS AND METHODS

Mouse strains

lulu was generated by ENU mutagenesis of C57/BL6J mice (García-García and Anderson, 2003; García-García et al., 2005; Kasarskis et al., 1998). The name *limulus* refers to the embryonic shape at E8.5, which resembles the horseshoe crab *Limulus polyphemos*. The *GT1* and *GT2* alleles of *Epb4.1l5* correspond to BayGenomics lines AE0088 and XC282, respectively. Embryonic stem (ES) cells were injected into C57BL/6J blastocysts to produce chimeras, which were screened for transmission of the gene trap. Carriers were genotyped by PCR amplification of the neomycin resistance gene using primer sets from the Jackson Laboratories.

Mapping and identification of *lulu*

lulu was mapped by backcrossing to C3HeB/FeJ, using linkage to flanking simple sequence length polymorphism (SSLP) markers from the MIT database or new markers that we generated (http://mouse.ski.mskcc.org/). *lulu* was mapped to a 650 kb interval by analyzing approximately 1000 informative recombination opportunities. The ENSEMBL and Celera databases were used for mapping and candidate gene selection; *Epb4.1l5*, *RalB* and *Ptpn4* were sequenced because of their predicted associations with the actin cytoskeleton. Complementary (c)DNAs of candidate genes were made from *lulu* mutant and C57BL/6J embryos using Superscript OneStep (Invitrogen). Products were subcloned into the Invitrogen pCR 2.1-TOPO vector and sequenced using T7 and SP6 primers. No sequence changes were found in the coding regions of *RalB* and *Ptpn4*; a single C to T transition was identified in the *Epb4.1l5* coding sequence, in multiple *lulu* mutant embryos. The *lulu* mutation abolishes a *Bsa*JI restriction site, which was used to confirm the mutation in carrier mice.

Phenotypic analysis

Whole-mount in situ hybridization, X-gal staining and immunohistochemistry were performed using standard protocols (Belo et al., 1997; Hogan et al., 1994; Yamada et al., 1993). All wild-type controls were littermates of the mutant embryos. Embryos were dissected in phosphate-buffered saline (PBS)/0.4% bovine serum albumin (BSA) and fixed in PBS/4% paraformaldehyde at 4°C overnight for in situ hybridization, or for 1 hour at room temperature for immunohistochemistry, with the exception that embryos used for N-cadherin staining were fixed for 10 minutes on ice in 100% methanol. Fixed embryos were embedded in OCT and cryosectioned at 8 μm thickness. Mutant and wild-type littermates were dissected and fixed together, and then embedded and sectioned in one block. Single slides containing wild-type and mutant sections were used for staining. Whole-mount embryos were imaged using a Zeiss Axiocam HRC digital camera on a Leica DM1RE2 inverted confocal microscope. Sections were imaged on a Leica MZFLIII microscope. In all cases, identical microscope and camera settings were used when imaging wild-type and mutant samples. Confocal datasets were analyzed using the Volocity software package (Improvision); 3D reconstructions were created using the Amira package (Mercury Computer Systems). The mitotic index was defined as the ratio of phospho-histone-H3-positive cells to total cells in anterior neural plate sections. Phospho-histone-H3-positive nuclei located 1 or more nuclear diameters away from the apical surface were scored as ectopic. Nuclear length and width were measured from 3D reconstructions.

Cell culture and cDNA transfections

HeLa cells were grown in Dulbecco's modified Eagle's medium (DMEM) supplemented with 10% fetal bovine serum. For transfection, cells were grown in six-well dishes and seeded onto glass coverslips at 60-70% confluency. pEGFP empty vector and *lulu*-pEGFP constructs were transfected into the cells using 1.5 μl of Lipofectamine 2000 and 0.5 μg of DNA per well in Opti-MeM. At 5 hours after transfection, the nucleotide-Lipofectamine mixture was removed and replaced with normal growth media. Immunocytochemistry was performed at approximately 24 hours after transfection.

Immunohistochemistry

The antigen used to produce the α-Lulu antibody, amino acids 669-731 of isoform B (Laprise et al., 2006), lies C-terminal to the stop codons in the *lulu*, *Epb4.1l5*^{GT1} and *Epb4.1l5*^{GT2} alleles. The α-crumbs homolog 3 (α-Crb3) antibody was raised against human CRB3 and recognizes all zebrafish Crumbs proteins (Hsu et al., 2006; Makarova et al., 2003); it is therefore likely to recognize all mouse Crumbs proteins. Other antibodies: rabbit α-Lulu antibody, 1:300 (Laprise et al., 2006); rabbit anti-Crb3, 1:250 (Makarova et al., 2003); rabbit anti-Sox2, 1:1000 (Chemicon); rabbit anti-phosphohistone H3, 1:200 (Upstate); rat anti-E-cadherin, 1:500 (Sigma); rabbit anti-Myosin IIB, 1:500 (Covance); rabbit anti-phospho-ERM, 1:50 (Cell Signaling); rabbit anti-laminin, 1:50 (Sigma); mouse anti-N-cadherin, 1:500 (BD Biosciences); mouse anti-ZO-2 (anti-Tjp2), 1:250 (BD Biosciences); rabbit anti-Pals1 (anti-Mpp5), 1:100 (Upstate); FITC- and TRITC-phalloidin, 10 U/ml (Molecular Probes).

Cells were fixed in 4% paraformaldehyde, 30 mM sucrose in PBS for 30 minutes at room temperature, permeabilized with 0.1% Triton X-100 and blocked with 2% normal donkey serum (Jackson ImmunoResearch Laboratories, West Grove, PA). Cells were incubated with a rhodamine-conjugated phalloidin (Invitrogen, Carlsbad, CA) for 30 minutes at 37°C. Confocal images were acquired using an LSM510 microscope (Carl Zeiss MicroImaging, Thornwood, NY). Quantification was based on counting 93 cells for both the pEGFP control and the pEGFP-*lulu* transfections and scoring cells that showed increased phalloidin staining at the cell cortex.

RESULTS

lulu mutant embryos arrest at E8.5 with defects in the morphogenesis of the mesoderm, endoderm and neural plate

The *lulu* mutation was identified because homozygous embryos showed striking morphological defects and arrested development at E8.5-9.0, prior to embryonic turning (García-García et al., 2005). *lulu* mutants had shortened trunks and lacked visible somites. The neural plate of E8.5 *lulu* embryos was raised in a series of transverse folds and failed to close to form the neural tube (Fig. 1A,B). Extra-embryonic tissues were also affected: the yolk sac appeared ruffled and the allantois did not fuse with the chorion (data not shown).

Mesoderm and definitive endoderm were specified, but abnormal, in *lulu* embryos. Analysis of molecular markers showed disruptions in axial, paraxial and cardiac mesoderm in *lulu* embryos. Brachyury (*T*) expression marks axial mesoderm and this gene was expressed discontinuously in the midline of E8.5 *lulu* mutants (Fig. 1E,F). *Meox1*, which marks somitic and presomitic mesoderm, was expressed in a greatly reduced, unsegmented domain in *lulu* mutants (Fig. 1G,H). *Nkx2.5* (also known as *Nkx2-5*), a marker for cardiac mesoderm, was expressed in the position of the lateral cardiac anlage; however, the lateral anlage failed to move to the midline to form a single heart tube (data not shown). In contrast to these tissues, the lateral plate mesoderm, assayed by *Twist1* expression, appeared normal in *lulu* embryos (data not shown). Definitive endoderm, marked by the expression of *Cerl* (also known as *Dand5*) at E7.5 and later by the gut markers *Hex1* (*Hhex*) and *Shh*, was also specified (data not shown). Despite normal specification, the endoderm failed to move ventrally to form the gut tube.

The broad anterior tissue of *lulu* mutants was identified as neural ectoderm, based on its expression of the pan-neural marker Sox2 (Fig. 1A,B). Despite its abnormal morphology, anterior-posterior

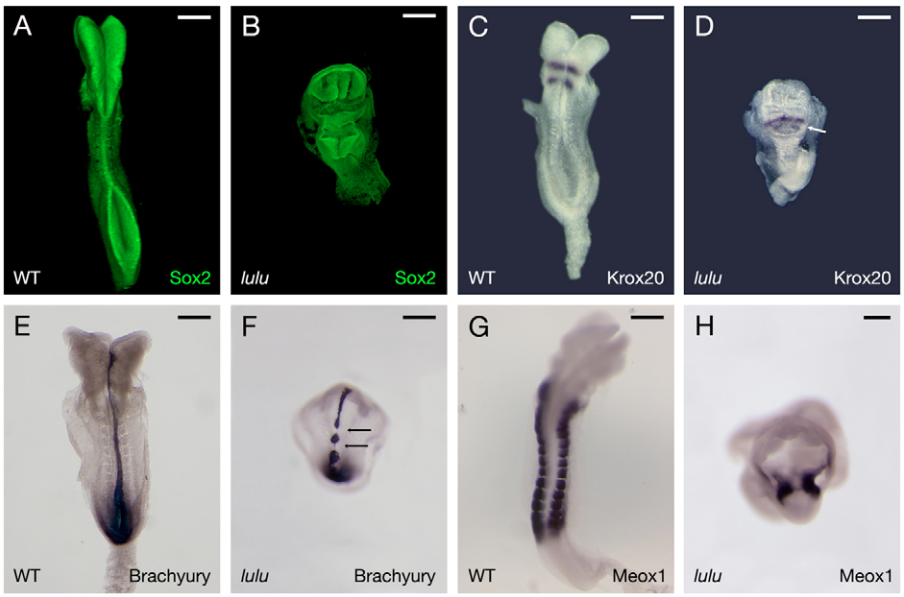

Fig. 1. Disruption of morphogenesis and maintenance of patterning in *lulu* mutants. Expression patterns at E8.5 assayed by immunofluorescence (**A**,**B**) or in situ hybridization (**C-H**). (A,B) 3D reconstructions from confocal *z*-stacks of wild-type (WT; A) and *lulu* (B) embryos stained with anti-Sox2 antibodies. (C,D) *Krox20* is expressed in rhombomeres 3 and 5 of the wild-type hindbrain (C), and in the *lulu* neural plate (D, arrow). (E,F) Brachyury (*T*) expression in the notochord is discontinuous in *lulu* (F, arrows). (G,H) *Meox1* expression in the paraxial mesoderm is unsegmented in *lulu* (H). All views are dorsal, except F, which is ventral. Anterior is up in all panels. Scale bars: 200 μm in A-D; 150 μm in E,F,H; 120 μm in G.

patterning of the neural plate was normal. *Krox20* (also known as *Egr2* – Mouse Genome Informatics), which marks rhombomeres 3 and 5 of the hindbrain, was expressed in two parallel stripes in the neural plate (Fig. 1C,D). Similarly, the anterior markers *Hesx1*, *Otx2*, *Wnt1* and *En1* were expressed in the correct anterior-posterior order (data not shown). Thus, the phenotypes seen in *lulu* mutant embryos appeared to reflect defects in morphogenesis rather than in cell type specification.

The *lulu* mutation inactivates the FERM-domain protein Epb4.1l5

The *lulu* mutation was mapped by meiotic recombination to a 650 kb interval of chromosome 1 that included the gene encoding the FERM-domain protein Epb4.1l5; we considered this to be a good candidate for *lulu* because other FERM-domain proteins connect the actin cytoskeleton to the cell surface and could therefore influence morphogenetic movements (Bretscher et al., 2002). We

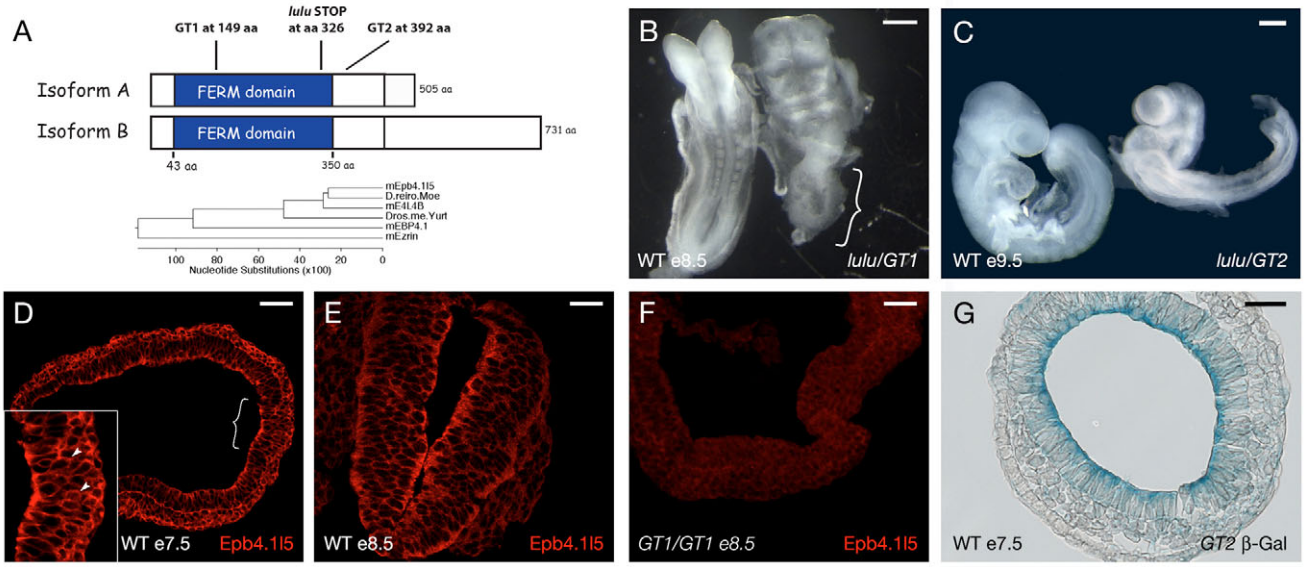

Fig. 2. Molecular identification of *lulu* and expression of Lulu protein. (**A**) Domain structure of Epb4.1l5, showing the *lulu* mutation site and the gene trap insertions. The FERM domain consists of amino acids (aa) 43 to 350. The cladogram shows FERM-domain relatedness among Lulu homologs and related mouse ERM proteins. (**B**) E8.5 *lulu/Epb4.1l5*^{GT1} transheterozygous mutant embryo (right; abnormal allantois, bracket), with its wild-type sibling (left). (**C**) *lulu/Epb4.1l5*^{GT2} transheterozygote (right) and wild-type sibling (left) at E9.5. (**D-F**) Anti-Lulu immunofluorescence on transverse sections of wild-type (D,E) and *Epb4.1l5*^{GT1} homozygous (F) embryos. Lulu is apically enriched in the E7.5 epiblast (D, arrowheads in inset) and E8.5 neural tube (E). Lulu is found at the periphery of cells ingressing in the primitive streak (D, bracket; inset is 2× magnification of the streak). (F) E8.5 neural plate from an *Epb4.1l5*^{GT1} homozygous embryo lacks detectable Lulu. (**G**) E7.5 transverse section of an *Epb4.1l5*^{GT2}/+ embryo, showing apical *GT2*–β-galactosidase activity. Anterior is up in B and left in C,D; dorsal is up in E,F. Scale bars: 150 μm in B,C; 50 μm in D,F,G; 20 μm in E.

identified a C to T transition mutation in *lulu* embryos that creates a premature stop codon near the C-terminal end of the FERM domain in *Epb4.1l5* (Fig. 2A). *Epb4.1l5* produces two alternatively spliced isoforms of 505 and 731 amino acids, which share a 444 amino acid N-terminal domain (including the entire FERM domain) but have divergent C-termini (Fig. 2A). The *lulu* mutation lies within the FERM domain and thus disrupts both isoforms. Mouse *lulu* is orthologous to the zebrafish *moe* gene, which encodes two isoforms of the same structure as *lulu* (Jensen and Westerfield, 2004) (www.ensembl.org). Yurt is the most closely related FERM-domain protein in *Drosophila*; its FERM domain is 68% identical to the Lulu FERM domain. The Yurt sequence C-terminal to the FERM domain is unrelated to Lulu; however, Yurt and both isoforms of Lulu terminate with putative PSD-95/Dlg/ZO-1 (PDZ)-binding motifs.

We confirmed the identity of *lulu* in complementation tests with two independent alleles of *Epb4.1l5* generated by BayGenomics (http://baygenomics.ucsf.edu). The *GT1* allele fuses the first 149 amino acids of Epb4.1l5 with β-galactosidase; the *GT2* allele creates a fusion of the first 392 amino acids, which includes the complete FERM domain, with β-galactosidase (Fig. 2A). *lulu/Epb4.1l5*^{GT1} transheterozygous embryos recapitulated the *lulu* phenotype, including a reduced trunk that lacked somites and a misshapen open neural plate (Fig. 2B). No full-length protein was detected by immunofluorescence or western blotting in either *lulu* or *Epb4.1l5*^{GT1} homozygous embryos (Fig. 2F and data not shown), indicating that there was no productive splicing around the gene trap vector. Because the early truncation in the *Epb4.1l5*^{GT1} allele produced the same phenotype as the *lulu* mutation, we infer that both are null alleles. The *Epb4.1l5*^{GT2} allele was hypomorphic: *lulu/Epb4.1l5*^{GT2} embryos arrested at E9.5, failed to complete embryonic turning, formed 10-12 pairs of abnormally shaped somites and partially closed the neural tube (Fig. 2C); *Epb4.1l5*^{GT2} homozygotes survived to E11.5 (data not shown). Because the data indicate that the *lulu* mutation inactivates the *Epb4.1l5* gene, we will refer to the product of the gene as the Lulu protein, for ease of pronunciation.

lulu (*Epb4.1l5*) mRNA was ubiquitously expressed at E7.5 and E8.5 (data not shown). Lulu protein was broadly expressed but was apically enriched in epithelial tissues (Fig. 2D,E). The apical concentration of Lulu mirrored that of the Epb4.1l5^{GT2}–β-galactosidase fusion protein, which contained an intact FERM domain and was also localized to the apical surface of embryonic epithelia (Fig. 2G). At gastrulation, Lulu protein localization shifted from an apical localization in the epiblast to a position around the circumference of ingressing cells (Fig. 2D, inset).

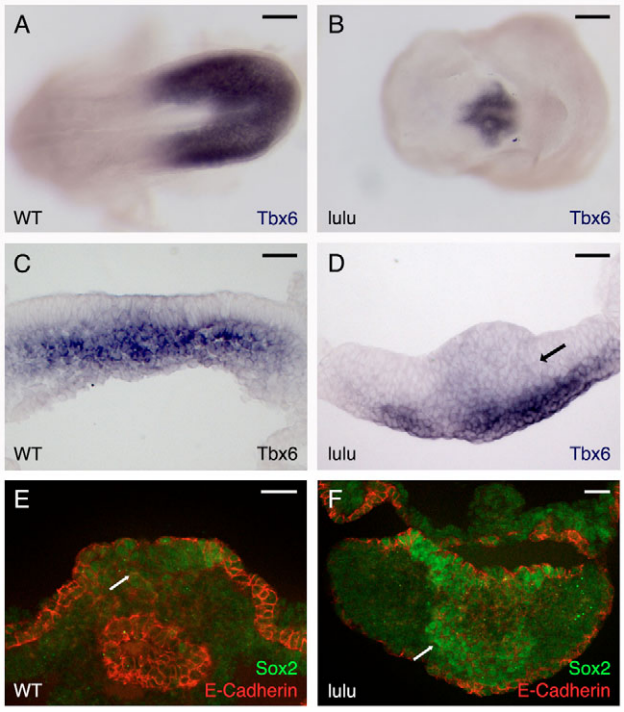

Fig. 3. Impaired paraxial mesoderm production in *lulu*. (**A-D**) Expression of *Tbx6* RNA in E8.5 wild-type (WT; A,C) and *lulu* (B,D) embryos, shown in whole mount (dorsal view in A, ventral in B) and transverse sections through the streak (C,D). (A,B) *Tbx6* expression flanks the streak and node in wild type (A); this domain is reduced in *lulu* mutants (B). (C,D) Cells accumulate under the streak in *lulu* mutants, producing a bulge of *Tbx6*-negative cells (D, arrow). (**E**,**F**) Immunofluorescence on transverse sections through the streak at E8.5. E-cadherin (red) and Sox2 (green) are maintained in cells underlying the streak in *lulu* mutants (F, arrow), but are lost in cells exiting the streak in wild type (E, arrow). Anterior is to the left in A,B; dorsal is up in C-F. Scale bars: 50 μm in A,B; 30 μm in C-F.

Lulu is important for the epithelial-to-mesenchymal transition at the primitive streak

One of the most striking aspects of the *lulu* phenotype was the deficit in paraxial mesoderm, seen in the dramatically reduced expression domains of *Meox1* (Fig. 1G,H) and of the presomitic mesoderm marker *Tbx6* (Fig. 3A,B). Mesoderm generation depends on successful completion of the EMT at the primitive streak. Downregulation of E-cadherin (also known as Cdh1 – Mouse Genome Informatics) is required for this EMT and for mesoderm migration away from the streak region (Burdsal et al., 1993; Ciruna and Rossant, 2001). Cells in the mesodermal layer of E7.5 *lulu* embryos correctly downregulated E-cadherin (Fig. 4A,B). However, transverse sections of the E8.5 streak showed that *lulu* embryos did have a defect in the EMT: although *Tbx6* was expressed in the nascent mesoderm beneath the primitive streak in both wild-type and *lulu* embryos (Fig. 3C,D), some mutant cells that had delaminated from the epithelial layer of the streak were located in an abnormal bulge in the region above the *Tbx6*-expressing mesoderm (Fig. 3D, arrow). The cells in the primitive streak bulge expressed E-cadherin and Sox2, two markers of the epiblast (Burdsal et al., 1993; Damjanov et al., 1986), although they did not have an epithelial morphology (Fig. 3E,F). Thus, although some *lulu* epiblast cells could undergo the EMT, downregulate E-cadherin and generate mesoderm, other cells at the *lulu* primitive streak apparently initiated the EMT but retained some epiblast character and were trapped in the streak.

Gastrulation appeared to initiate normally in *lulu* embryos, but defects in the primitive streak could be detected in phalloidin-stained embryos by E7.75. By this stage, mesoderm had spread around the embryonic circumference in *lulu* embryos, as in wild type (Fig. 4C,D), but the anterior mesodermal wings were only a single cell thick, in contrast to three to four cells thick in wild-type littermates (Fig. 4E,F). This suggested that, by E7.75, the number of mesodermal cells was already reduced, but that mutant mesodermal cells that escaped the streak region could migrate effectively. The ability of mutant mesoderm cells to migrate was confirmed in E7.5 primitive streak explants, where *lulu* mutant mesoderm cells migrated efficiently away from the streak (data not shown).

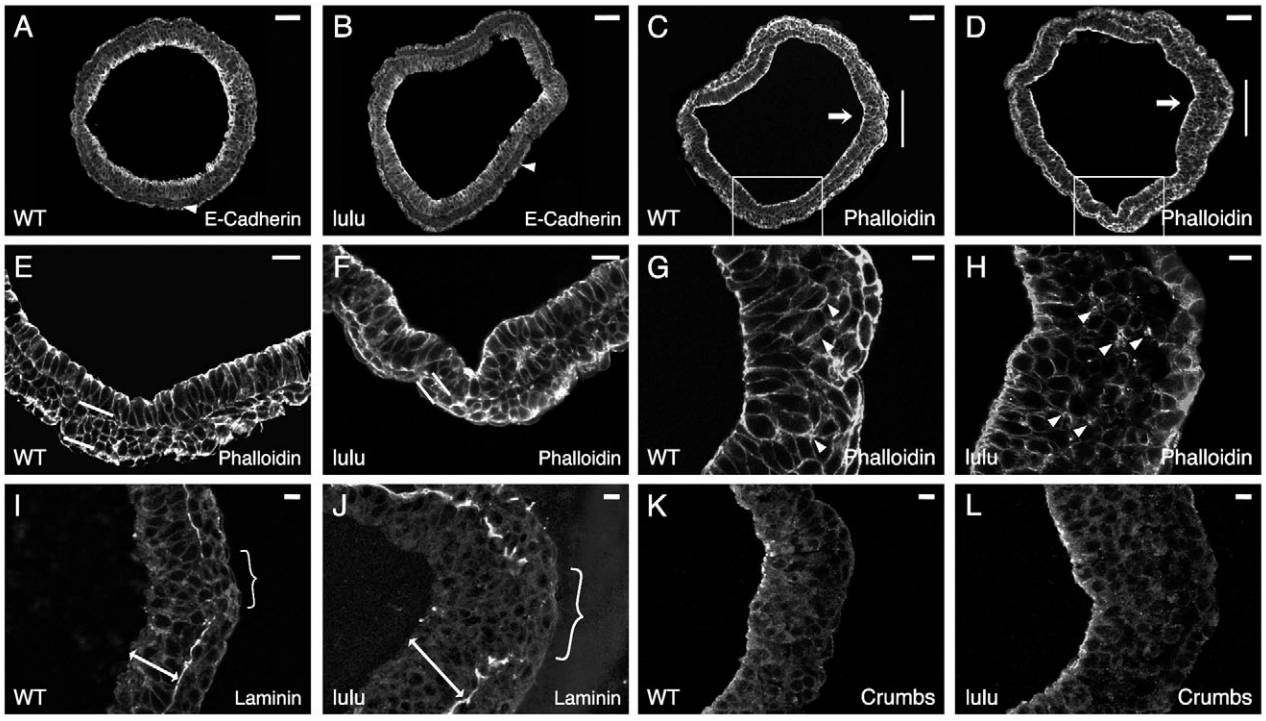

Fig. 4. Defective EMT in the *lulu* primitive streak. E7.5 (**A**,**B**) and E7.75 (**C-L**) transverse sections of wild-type (WT; A,C,E,G,I,K) and *lulu* (B,D,F,H,J,L) embryos. (A,B) In wild-type and *lulu* embryos, E-cadherin is expressed in the epiblast but is downregulated in the mesodermal wings (arrowheads). (C-H) Phalloidin labels F-actin. Arrows in C,D mark the primitive streak; boxes are magnified in E,F; bars mark the regions magnified in G,H. Mesodermal wings are thicker in wild type than in *lulu* mutants (bars; E,F). F-actin is evenly distributed around delaminating cells in the wild-type streak (arrowheads, G), whereas cells in the *lulu* streak show spots of bright punctate F-actin staining (arrowheads, H). (I,J) Anti-laminin staining marks the epiblast basal lamina and highlights the increased width of the *lulu* streak compared with wild type (brackets). The epiblast near the streak is also thicker in *lulu* mutants (double-headed arrows). (K,L) Crumbs proteins are apically concentrated in the wild-type (K) and *lulu* (L) epiblast but are absent in involuting mesoderm. Anterior is to the left in A-D; apical is up in E,F and to the left in G-L. Scale bars: 50 μm in A-D; 10 μm in E-L.

The primitive streak of E7.75 *lulu* embryos was thicker and wider than the wild-type streak (Fig. 4C,D,G,H). Laminin marks the basement membrane that separates the epiblast and mesoderm, and there is a gap in laminin staining at the position of the wild-type primitive streak (Fig. 4I, bracket). In *lulu* mutants, the gap in laminin expression was wider than in the wild type (Fig. 4J, bracket). Laminin staining also highlighted the increased thickness of the E7.75 streak in *lulu* mutants compared with wild type (Fig. 4I,J, arrows), similar to the increased thickness that was seen at E8.5 (Fig. 3D).

It has been shown that mouse Lulu can bind all three mammalian Crumbs proteins (CRB1-CRB3), and that its *Drosophila* homolog is required for normal apical localization of *Drosophila* Crumbs (Laprise et al., 2006). Therefore, it was possible that the EMT defect in *lulu* might represent a disruption of apical-basal polarity. We examined the expression of Crumbs proteins at the primitive streak using a pan-Crumbs antibody (Hsu et al., 2006; Makarova et al., 2003). In both wild-type and *lulu* embryos, Crumbs proteins were expressed apically in the epiblast at E7.5, and were absent from nascent mesoderm cells (Fig. 4K,L). Crumbs proteins were not detected in the cells that accumulated in the abnormal bulge at the *lulu* streak, which indicated that these cells had lost this characteristic of the epiblast. These results show that Lulu is required neither for apical localization of Crumbs in the epiblast nor for the downregulation of Crumbs in nascent mesoderm.

Phalloidin staining of E7.5 embryos revealed defects in actin organization in the mutant primitive streak. In the wild-type primitive streak, F-actin was enriched around the periphery of cells that were ingressing through the streak (Fig. 4G, arrowheads), in a pattern remarkably similar to the distribution of Lulu protein (Fig. 2D). By contrast, the circumferential F-actin was not present in cells of the *lulu* streak; instead, puncta of F-actin were prominent in the cells that accumulated in the *lulu* streak at E7.5 (Fig. 4H, arrowheads) and E8.5 (data not shown). Because some FERM-domain proteins bind actin (Bretscher et al., 2002), this abnormal distribution of F-actin could represent the primary defect that prevents the normal EMT in the *lulu* primitive streak.

Abnormal organization of the *lulu* anterior neural plate

The other tissue with particularly striking defects in *lulu* embryos was the neural plate. The anterior neural plate of *lulu* embryos was broad, open and folded into irregular ridges (Fig. 1B,D), and it appeared thicker than the wild-type neural plate (Fig. 5A,B). To evaluate whether the apparently large size of the neural plate could reflect excessive proliferation in that tissue, we counted the total number of cells in the anterior neural plate. Sox2 is expressed in the pseudo-stratified neural ectoderm and the columnar gut endoderm, whereas E-cadherin is expressed in the gut endoderm and the cuboidal surface ectoderm (Fig. 5A,B); therefore neural cells were defined as Sox2-positive and E-cadherin-negative ($Sox2^+$, E-$cadherin^-$). The total number of $Sox2^+$, E-$cadherin^-$ cells in the anterior *lulu* neural plate was approximately the same as in wild-type littermates (Table 1). We also assayed the fraction of neural cells in mitosis, based on staining with anti-phospho-histone H3 antibodies

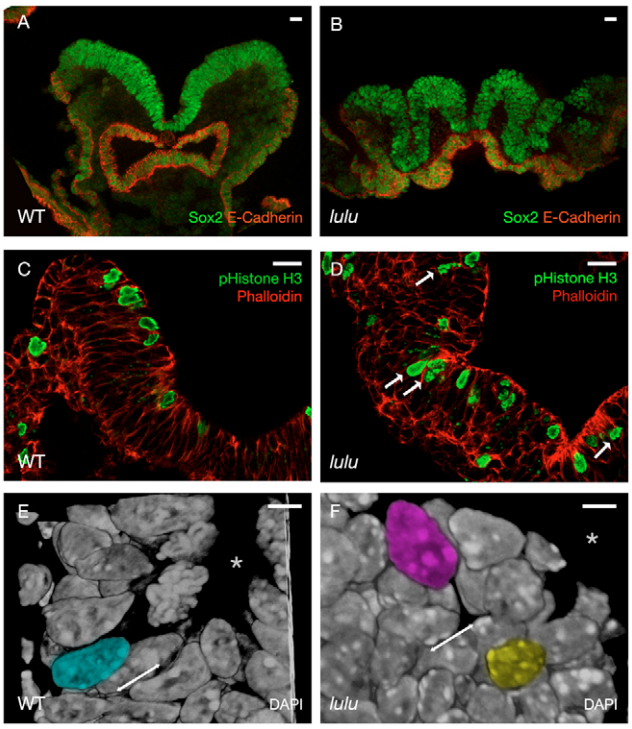

Fig. 5. Morphogenetic defects in the *lulu* neural plate. (**A-D**) Transverse sections of E8.5 wild-type (WT; A,C) and *lulu* mutant (B,D) embryos. (A,B) Sox2 antibody (green) labels the pseudo-stratified neural plate (dorsal) and the columnar gut endoderm (ventral). E-cadherin (red) labels the gut endoderm and the cuboidal surface ectoderm lateral to the neural plate. The neural plate in *lulu* mutants appears thickened and broader than in wild type, and the foregut fails to close. (C,D) Phospho-histone H3 (green)-labeled mitotic nuclei are apical in wild type (C); some mitotic nuclei are not apical in *lulu* (arrows, D). Phalloidin (red) shows cell shape. (**E**,**F**) 3D reconstructions of DAPI-stained nuclei (representatives false-colored) in wild-type (E) and *lulu* (F) anterior neural plates; the apical surface (asterisks) and apical-basal axis (double-headed arrows) are indicated. Wild-type nuclei (E) are ellipsoid and align with the apical-basal axis (cyan nucleus). *lulu* nuclei (F) vary in shape (spherical nucleus, yellow) and appear to align randomly (magenta nucleus). Dorsal is up in all panels. Scale bars: 20 μm in A-D; 5 μm in E,F.

(Fig. 5C,D and Table 1). The mitotic index in the *lulu* anterior neural plate was indistinguishable from that of wild type (Table 1). We conclude that the abnormal shape of the neural plate in *lulu* embryos is not caused by abnormal proliferation or by an increase in the number of neural cells; instead, the abnormal shape represents a defect in the organization of the neural tissue.

The nuclei of *lulu* neural cells appeared to be rounder than wild type (Fig. 5A,B). Nuclear shape varies with cell shape, which is a function of the cytoskeleton. Because of the dense cell packing within the pseudo-stratified neuroepithelium, we were unable to examine cell shape directly by using cell surface labeling. We therefore examined nuclear morphology as an indicator of cell shape, using DAPI staining of the nuclei and 3D reconstructions of confocal *z*-stacks through the neural plates of wild-type and *lulu* embryos. Whereas wild-type neural plate nuclei were ellipsoid and elongated along the apical-basal axis, with an average length:width ratio of 2.33 (Fig. 5E, Table 1), *lulu* neural plate nuclei were more spherical, with an average length:width ratio of 1.44, and many of the ellipsoid nuclei did not align their long axes with the apical-basal axis (Fig. 5F, Table 1). Thus, there appears to be a global distortion of nuclear shape and orientation within the *lulu* neural plate.

Although the mitotic index in the *lulu* neural plate was normal, phospho-histone H3 staining revealed another defect in the organization of the neural epithelium (Fig. 5C,D). Nuclei in columnar and pseudo-stratified epithelia, such as the neural plate, migrate along the apical-basal axis of the cell during the cell cycle, and mitosis takes place when nuclei are at the apical surface (Götz and Huttner, 2005). We observed that 20% of phospho-histone H3-positive nuclei in the *lulu* neuroepithelium were located away from the apical surface (Fig. 5D, arrows), whereas only 5% of phospho-histone H3-positive nuclei were located away from the apical surface in the wild-type neural plate (Table 1).

Markers of apical junctions are localized correctly in the *lulu* neural plate

It was possible that the abnormally positioned mitoses in the *lulu* neural plate reflected a defect in the apical-basal polarity of the epithelium, which depends on the proper organization of apical junctions (Imai et al., 2006; Koike et al., 2005; Wei and Malicki, 2002). We therefore examined the organization of tight junctions and adherens junctions in the *lulu* neural plate. We found that the tight junction transmembrane proteins occludin and claudin 1, as well as the tight junction-associated proteins ZO-1 (Tjp1) and ZO-2 (Tjp2), were expressed and apically localized in *lulu* mutant neural plates (Fig. 6A,B and data not shown). N-cadherin, the major cadherin present in the neuroepithelium (Radice et al., 1997), and its associated protein, β-catenin, were also enriched in the apical neural plate of both wild-type and *lulu* E8.5 embryos (Fig. 6C,D and data not shown).

Because Lulu can bind Crumbs proteins (Hsu et al., 2006; Jensen and Westerfield, 2004; Laprise et al., 2006; Omori and Malicki, 2006), we tested whether components of the Crumbs complex were localized normally in the *lulu* neural plate. Crumbs proteins were detected at the apical surface of the neuroepithelium in wild-type, *lulu* and *Epb4.115*^{GT1} homozygous embryos (Fig. 6E,F and data not shown). Pals1 (also known as Mpp5 – Mouse Genome Informatics), a MAGUK protein that binds Crumbs and the zebrafish Lulu ortholog, Moe (Hsu et al., 2006), was expressed on the apical surface, as well as in part of the lateral surface between adjacent cells, in both the wild-type and the *lulu* neural plate (Fig. 6G,H). The Par6-Par3-aPKC (aPKC is also known as Prkci – Mouse Genome Informatics) complex interacts with the Crumbs complex (Hurd et al., 2003; Lemmers et al., 2004); we found that Par3 was present

Table 1. Quantification of neural plate size, mitosis and nuclear shape in wild-type and *lulu* embryos

	Total neural cells	Mitotic index (%)	Ectopic pH3$^+$ nuclei (%)	Average L/W ratio
Wild type	25,315	5.35 (390/7295)	5.45 (27/495)	2.33±0.45 (*n*=100)
lulu	23,205	5.32 (373/7013)	19.92 (47/236)	1.44±0.29 (*n*=78)

Total anterior neural cells at E8.5 were counted and averaged for two wild-type and three *lulu* mutant embryos. The mitotic index [phospho-histone-H3-positive (pH3$^+$) nuclei/total nuclei] was unchanged in *lulu* mutants. However, there was a 3.6-fold increase in ectopic mitotic nuclei in *lulu* embryos. Nuclear length:width (L/W) ratio was defined as the longest axis of the nucleus (L) divided by the orthogonal axis (W). ±, 1 standard deviation.

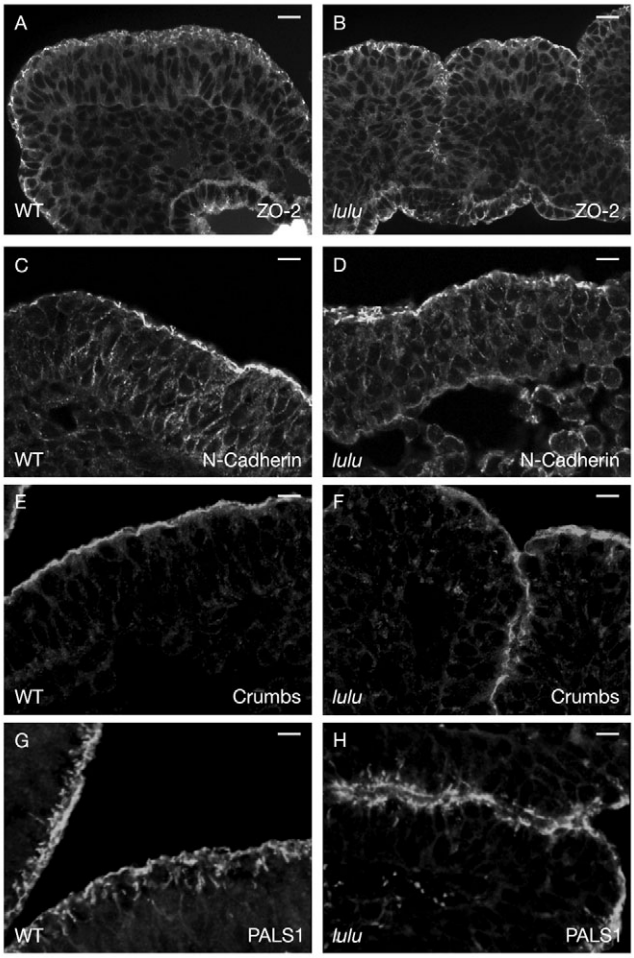

Fig. 6. Apical markers are correctly localized in the *lulu* neural plate. (**A-H**) Immunofluorescence on transverse sections of E8.5 wild-type (WT; A,C,E,G) and *lulu* mutant (B,D,F,H) neural plates. (A,B) ZO-2 marks the tight junctions at the apical-basal border of the neuroepithelium. (C,D) N-cadherin marks adherens junctions. (E,F) Crumbs is restricted to the apical surface. (G,H) Pals1 is localized to the apical and apico-lateral domain. Dorsal is up in all panels. Scale bar: 10 μm in A,B; 5 μm in C-H.

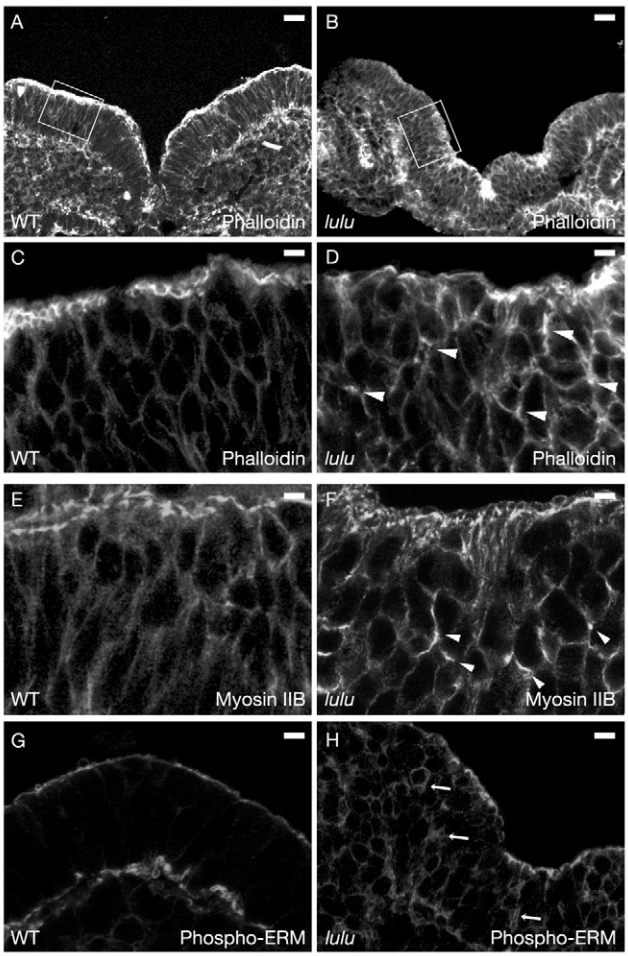

Fig. 7. Cytoskeletal alterations in the *lulu* neural plate. (**A-H**) Transverse sections of E8.5 wild-type (WT; A,C,E,G) and *lulu* (B,D,F,H) anterior neural plates; boxes in A,B show the equivalent positions of the high-magnification images in C,E,G and D,F,H, respectively. (A-D) Phalloidin reveals F-actin localization and tissue shape; ectopic concentrations of F-actin appear away from the apical surface of the *lulu* neuroepithelium (arrowheads, D). (E,F) Myosin IIB is concentrated at ectopic sites in the *lulu* neural plate (arrowheads, F). (G,H) Anti-phospho-ERM antibody recognizes activated (actin-binding) ERM proteins; *lulu* neural plates show ectopic phospho-ERM staining away from the apical surface. Scale bars: 25 μm in A,B; 5 μm in C-F; 10 μm in G,H.

apically in both the wild-type and *lulu* neural plate (data not shown). Thus, these markers of apical-basal polarity appeared to be localized correctly in the *lulu* neural plate.

Lulu is required for normal organization of the actin cytoskeleton in the neural plate

Because many previously studied FERM proteins bind actin (Bretscher et al., 2000; Tsukita and Yonemura, 1999) and because we observed ectopic F-actin in the *lulu* primitive streak, we examined the organization of F-actin in the *lulu* neural epithelium. In wild-type E8.5 neural plate, phalloidin staining showed that F-actin formed a dense band near the apical surface of each cell (Fig. 7A,C). By contrast, although F-actin was enriched apically in the *lulu* neural plate, it was also present ectopically at more basal positions (Fig. 7B,D, arrowheads). Myosin IIB is a major non-muscle myosin and participates in apical constriction of the actin ring, an essential step during neural tube closure (Haigo et al., 2003; Hildebrand, 2005). Myosin IIB was highly enriched at the apical surface of the wild-type neural plate (Fig. 7E). By contrast, Myosin IIB was seen both apically and in ectopic basal positions in the *lulu* neural plate (Fig. 7F, arrowheads). Spnb2 (βII-spectrin), an F-actin-binding protein (Liu et al., 1987), showed similar ectopic staining within the neuroepithelium (data not shown). Phospho-ERM (P-ERM) antibodies, which recognize the activated, F-actin-binding forms of ezrin, radixin and moesin (Gary and Bretscher, 1995; Matsui et al., 1998), strongly labeled the apical surface of the wild-type neural plate (Fig 7G), consistent with previous reports of their apical localization in other epithelia (Berryman et al., 1993; Morales et al., 2004). By contrast, P-ERM was found both apically and more basally in the neuroepithelium of *lulu* mutants (Fig. 7H), which again indicated the presence of ectopic F-actin at basal positions in the *lulu* neural epithelium.

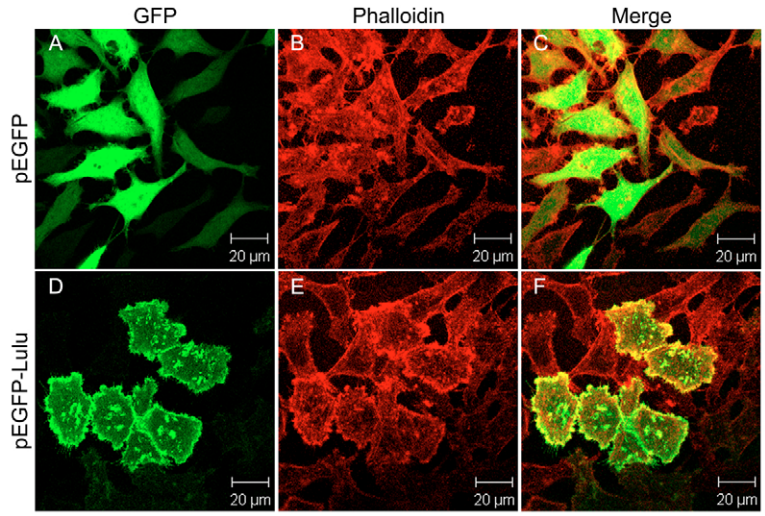

Fig. 8. Expression of Lulu alters the actin organization of HeLa cells. HeLa cells transfected with either pEGFP alone (**A-C**) or pEGFP-*lulu* (**D-F**) were grown on glass coverslips, fixed, permeabilized and stained with phalloidin (red). pEGFP-Lulu localized to the plasma membrane and colocalized with increased phalloidin staining at the cell cortex. Scale bars: 20 μm.

To investigate whether Lulu might regulate the actin cytoskeleton directly, we expressed EGFP-tagged Lulu protein in HeLa cells. EGFP-Lulu was concentrated at the plasma membrane and we observed increased phalloidin staining at the cell cortex in 66% of the transfected cells, whereas only 30% of EGFP-control transfected cells had phalloidin staining concentrated at the cell periphery (Fig. 8). In addition, compared with the transfected control cells, the HeLa cells that overexpressed EGFP-Lulu appeared more spread out and showed increased numbers of small actin-rich protrusions. Thus, overexpression of Lulu was sufficient to increase cortical actin and alter the morphology of these epithelial cells.

DISCUSSION

Lulu is essential for early mammalian development

The results presented here demonstrate that the mouse FERM-domain protein Lulu has a central role in the morphogenesis of the early mouse embryo. Embryos that lack Lulu die before mid-gestation, with a syndrome of developmental defects that affects all three germ layers. The *lulu* phenotype is much more severe than that of its zebrafish homolog, *moe*: null *moe* mutations allow survival to the end of embryogenesis, and the only defects that have been reported in *moe* mutants are in retinal lamination and in brain ventricle size (Jensen et al., 2001; Jensen and Westerfield, 2004). The milder *moe* phenotype could reflect the large contribution of maternal gene products to zebrafish development, although translation-blocking morpholinos recapitulate the *moe* mutations (Jensen and Westerfield, 2004). Alternatively, the cellular behaviors required for gastrulation and neural tube formation are distinct in zebrafish and mouse (Adams and Kimmel, 2004; Geldmacher-Voss et al., 2003) and may depend on different molecular machines.

Lulu acts at an intermediate step in the epithelial-mesenchymal transition

The absence of Lulu leads to dramatic defects in the production and morphogenesis of paraxial mesoderm, including the complete absence of somites. Some mesoderm forms in the absence of Lulu, but fewer cells are present in the mesodermal wings as soon as they surround the embryo. These defects are the consequence of the abnormal organization of the primitive streak, where cells begin to accumulate as early as E7.5.

During the EMT at the primitive streak, cells must lose epithelial cell junctions, escape the epithelial layer and acquire the properties of mesenchymal cells (Shook and Keller, 2003). These morphological transitions are accompanied by changes in gene expression, as cells downregulate expression of epithelial genes, such as *Sox2* and E-cadherin, and upregulate mesodermal genes, such as *Tbx6*. The early steps of the EMT (breakdown of the basement membrane, loss of cell-cell junctions and downregulation of Crumbs) do not require Lulu. However, in the absence of Lulu, many cells accumulate at the primitive streak. Although these abnormal streak cells have lost their epithelial organization, they continue to express the epithelial markers Sox2 and E-cadherin, and do not express the mesodermal marker *Tbx6*. Thus, these *lulu* mutant cells appear to be trapped at an intermediate state in the EMT.

Mutations in *Fgfr1*, *Snail* (also known as *Snai1*) and *p38IP* (also known as D3Ertd300e) all block the gastrulation EMT and, in each case, the defect has been attributed to the inability to downregulate expression of E-cadherin (Ciruna and Rossant, 2001; Carver et al., 2001; Zohn et al., 2006). By contrast, although E-cadherin is expressed in the cells trapped at the *lulu* primitive streak, E-cadherin is downregulated in the mesodermal wings in *lulu* mutant embryos (Fig. 4B). This suggests that the *lulu* phenotype defines a previously unrecognized step of the EMT that requires a Lulu-dependent reorganization of the actin cytoskeleton. The change in Lulu protein localization during the EMT suggests that it plays an active role in the EMT: Lulu is enriched at the apical surface of the epiblast and then relocalizes to the periphery of ingressing cells. This change in localization parallels the rearrangements seen in F-actin, which is also apically localized in the epiblast and surrounds the ingressing cells in the streak. In *lulu* mutants, this rearrangement of F-actin fails and, instead, cells in the mutant streak show ectopic foci of F-actin. We therefore propose that Lulu helps anchor F-actin to the surface of ingressing cells and that the architecture of the cells at this transition state is important for the changes in adhesion and motility that allow these cells to acquire a mesenchymal character. Some FERM domains have been shown to bind F-actin (Bretscher et al., 2002), and overexpressed Lulu is sufficient to reorganize the morphology and actin cytoskeleton in HeLa cells (Fig. 8). We therefore suggest that Lulu regulates the F-actin cytoskeleton during the EMT, either via the direct binding of actin or via an intermediary protein.

Lulu and the organization of the neural epithelium

The second striking defect in *lulu* mutant embryos is that the anterior neural plate is broader and thicker than wild type; the irregular folding pattern in *lulu* mutants is strikingly different than the median and dorsolateral folds that lead to wild-type neural tube closure. These defects are not due to differences in cell proliferation or cell number, nor are they due to a loss of the apical junctions that are a hallmark of the apical domain of epithelial cells. Instead, we observe that the abnormal morphology of the neural plate is coupled to defects in organization of the apical actin network: F-actin and F-actin-binding proteins are present at basal positions in the epithelium of the anterior neural plate, in addition to their normal apical location.

Mouse Lulu, like its *Drosophila* and zebrafish homologs, binds Crumbs proteins, which are key determinants of the apical domain of epithelial cells (Laprise et al., 2006). Recent work in both *Drosophila* and zebrafish has indicated that the function of these Lulu homologs is to regulate the size of the apical domain of epithelial cells via regulation of either the localization or the activity of Crumbs (Hsu et al., 2006; Laprise et al., 2006). The effect of the loss of *Drosophila* Yurt varies between tissues: in the ventral ectoderm, the domain of Crumbs expression is expanded in *yurt* mutants, while, in *yurt* mutant photoreceptors, the apical domain is expanded in a Crumbs-dependent fashion without a change in the domain of Crumbs expression (Laprise et al., 2006). Loss of zebrafish *moe* function prevents tight junctions from forming in the retina (Jensen and Westerfield, 2004), possibly due to loss of apical Crumbs proteins in the *moe* retina (Hsu et al., 2006). In contrast to these results, we find that loss of Lulu does not affect Crumbs localization or apical junction formation (Fig. 6), and en-face imaging did not reveal differences in the size of the apical domain of mutant cells in the neural epithelium (data not shown).

The *lulu* neural plate does not have detectable defects in apical junctions, but does show a clear disruption in the organization of the apical F-actin network. One possible explanation for these findings is that the loss of Lulu leads to a partial disruption in apical-basal polarity, so that some cells lose their connections to the apical surface of the pseudo-stratified neural epithelium and the F-actin network associated with these cells appears as ectopic, basal F-actin. However, the disruption of cellular organization in the neural epithelium does not appear to be limited to a sub-population of neural cells. For example, P-ERM, which marks apical F-actin, is ectopically localized throughout the mutant neural epithelium. Similarly, the nuclei throughout the mutant neural epithelium are less elongated than wild type and are not correctly oriented with respect to the apical-basal axis of epithelium (Fig. 5F, Table 1), which is likely to reflect a general change in cellular architecture. Thus, we conclude that there is a global disruption of cell organization in the *lulu* neural plate.

We suggest that Lulu is required to link the F-actin cytoskeleton to plasma-membrane protein complexes that are important during the dynamic cell rearrangements that take place during both the EMT at gastrulation and the folding of the neural plate. One model that reconciles the demonstrated ability of Crumbs to bind Lulu with our findings would be that mouse Crumbs acts upstream of Lulu, and Lulu helps to link Crumbs to the actin cytoskeleton. Alternatively, Lulu may act independently of Crumbs to anchor the F-actin cytoskeleton as it rearranges or contracts. In the future, characterization of the functions of the mouse Crumbs complex proteins and of genes that produce *lulu*-like phenotypes (García-García et al., 2005) should distinguish among these possibilities.

We thank the Sloan-Kettering transgenic facility for production of the *lulu* gene trap mice, and the Sloan-Kettering molecular cytology core facility for expert technical assistance during confocal imaging. We thank B. Margolis for the Crb3 antibody; and M. Baylies, J. Zallen, S. Shi and the Anderson laboratory for comments on the manuscript. *Epb4.1l5*^{GT1} and *Epb4.1l5*^{GT2} ES cells were obtained from BayGenomics. Genome sequence analysis used ENSEMBL and the Celera Discovery System and associated databases. J.D.L. was supported by an NRSA, and N.F.S-G by a postdoctoral fellowship from the Foundation Fighting Blindness Canada. The work was supported by the National Institutes of Health grant HD35455 to K.V.A. and a grant from the Foundation Fighting Blindness Canada to C.J.M.

References

Adams, R. and Kimmel, C. (2004). Morphogenetic cellular flows during Zebrafish gastrulation. In *Gastrulation: From Cells to Embryo* (ed. C. D. Stern), pp. 305-316. Cold Spring Harbor: Cold Spring Harbor Laboratory Press.

Belo, J. A., Bouwmeester, T., Leyns, L., Kertesz, N., Gallo, M., Follettie, M. and De Robertis, E. M. (1997). Cerberus-like is a secreted factor with neutralizing activity expressed in the anterior primitive endoderm of the mouse gastrula. *Mech. Dev.* **68**, 45-57.

Berryman, M., Franck, Z. and Bretscher, A. (1993). Ezrin is concentrated in the apical microvilli of a wide variety of epithelial cells whereas moesin is found primarily in endothelial cells. *J. Cell Sci.* **105**, 1025-1043.

Bretscher, A., Chambers, D., Nguyen, R. and Reczek, D. (2000). ERM-Merlin and EBP50 protein families in plasma membrane organization and function. *Annu. Rev. Cell Dev. Biol.* **16**, 113-143.

Bretscher, A., Edwards, K. and Fehon, R. G. (2002). ERM proteins and merlin: integrators at the cell cortex. *Nat. Rev. Mol. Cell Biol.* **3**, 586-599.

Burdsal, C. A., Damsky, C. H. and Pedersen, R. A. (1993). The role of E-cadherin and integrins in mesoderm differentiation and migration at the mammalian primitive streak. *Development* **118**, 829-844.

Carver, E. A., Jiang, R., Lan, Y., Oram, K. F. and Gridley, T. (2001). The mouse snail gene encodes a key regulator of the epithelial-mesenchymal transition. *Mol. Cell. Biol.* **21**, 8184-8188.

Ciruna, B. and Rossant, J. (2001). FGF signaling regulates mesoderm cell fate specification and morphogenetic movement at the primitive streak. *Dev. Cell* **1**, 37-49.

Damjanov, I., Damjanov, A. and Damsky, C. H. (1986). Developmentally regulated expression of the cell-cell adhesion glycoprotein cell-CAM 120/80 in peri-implantation mouse embryos and extraembryonic membranes. *Dev. Biol.* **116**, 194-202.

García-García, M. J. and Anderson, K. V. (2003). Essential role of glycosaminoglycans in Fgf signaling during mouse gastrulation. *Cell* **114**, 727-737.

García-García, M. J., Eggenschwiler, J. T., Caspary, T., Alcorn, H. L., Wyler, M. R., Huangfu, D., Rakeman, A. S., Lee, J. D., Feinberg, E. H., Timmer, J. R. et al. (2005). Analysis of mouse embryonic patterning and morphogenesis by forward genetics. *Proc. Natl. Acad. Sci. USA* **102**, 5913-5919.

Gary, R. and Bretscher, A. (1995). Ezrin self-association involves binding of an N-terminal domain to a normally masked C-terminal domain that includes the F-actin binding site. *Mol. Biol. Cell* **6**, 1061-1075.

Geldmacher-Voss, B., Reugels, A. M., Pauls, S. and Campos-Ortega, J. A. (2003). A 90-degree rotation of the mitotic spindle changes the orientation of mitoses of zebrafish neuroepithelial cells. *Development* **130**, 3767-3780.

Götz, M. and Huttner, W. B. (2005). The cell biology of neurogenesis. *Nat. Rev. Mol. Cell Biol.* **6**, 777-788.

Haigo, S. L., Hildebrand, J. D., Harland, R. M. and Wallingford, J. B. (2003). Shroom induces apical constriction and is required for hingepoint formation during neural tube closure. *Curr. Biol.* **13**, 2125-2137.

Hildebrand, J. D. (2005). Shroom regulates epithelial cell shape via the apical positioning of an actomyosin network. *J. Cell Sci.* **118**, 5191-5203.

Hogan, B. L., Blessing, M., Winnier, G. E., Suzuki, N. and Jones, C. M. (1994). Growth factors in development: the role of TGF-beta related polypeptide signalling molecules in embryogenesis. *Dev. Suppl.* **1994**, 53-60.

Hoover, K. B. and Bryant, P. J. (2002). Drosophila Yurt is a new protein-4.1-like protein required for epithelial morphogenesis. *Dev. Genes Evol.* **212**, 230-238.

Hsu, Y., Willoughby, J. J., Christensen, A. K. and Jensen, A. M. (2006). Mosaic eyes is a novel component of the crumbs complex and negatively regulates photoreceptor apical size. *Development* **133**, 4849-4859.

Hurd, T. W., Gao, L., Roh, M. H., Macara, I. G. and Margolis, B. (2003). Direct interaction of two polarity complexes implicated in epithelial tight junction assembly. *Nat. Cell Biol.* **5**, 137-142.

Imai, F., Hirai, S., Akimoto, K., Koyama, H., Miyata, T., Ogawa, M., Noguchi, S., Sasaoka, T., Noda, T. and Ohno, S. (2006). Inactivation of aPKC{lambda} results in the loss of adherens junctions in neuroepithelial cells without affecting neurogenesis in mouse neocortex. *Development* **133**, 1735-1744.

Jensen, A. M. and Westerfield, M. (2004). Zebrafish mosaic eyes is a novel FERM protein required for retinal lamination and retinal pigmented epithelial tight junction formation. *Curr. Biol.* **14**, 711-717.

Jensen, A. M., Walker, C. and Westerfield, M. (2001). mosaic eyes: a zebrafish gene required in pigmented epithelium for apical localization of retinal cell division and lamination. *Development* **128**, 95-105.
Kasarskis, A., Manova, K. and Anderson, K. V. (1998). A phenotype-based screen for embryonic lethal mutations in the mouse. *Proc. Natl. Acad. Sci. USA* **95**, 7485-7490.
Koike, C., Nishida, A., Akimoto, K., Nakaya, M. A., Noda, T., Ohno, S. and Furukawa, T. (2005). Function of atypical protein kinase C lambda in differentiating photoreceptors is required for proper lamination of mouse retina. *J. Neurosci.* **25**, 10290-10298.
Laprise, P., Beronja, S., Silva-Gagliardi, N. F., Pellikka, M., Jensen, A. M., McGlade, C. J. and Tepass, U. (2006). The FERM protein yurt is a negative regulatory component of the crumbs complex that controls epithelial polarity and apical membrane size. *Dev. Cell* **11**, 363-374.
Lemmers, C., Michel, D., Lane-Guermonprez, L., Delgrossi, M. H., Medina, E., Arsanto, J. P. and Le Bivic, A. (2004). CRB3 binds directly to Par6 and regulates the morphogenesis of the tight junctions in mammalian epithelial cells. *Mol. Biol. Cell* **15**, 1324-1333.
Liu, S. C., Derick, L. H. and Palek, J. (1987). Visualization of the hexagonal lattice in the erythrocyte membrane skeleton. *J. Cell Biol.* **104**, 527-536.
Makarova, O., Roh, M. H., Liu, C. J., Laurinec, S. and Margolis, B. (2003). Mammalian Crumbs3 is a small transmembrane protein linked to protein associated with Lin-7 (Pals1). *Gene* **302**, 21-29.
Mangeat, P., Roy, C. and Martin, M. (1999). ERM proteins in cell adhesion and membrane dynamics. *Trends Cell Biol.* **9**, 187-192.
Matsui, T., Maeda, M., Doi, Y., Yonemura, S., Amano, M., Kaibuchi, K., Tsukita, S. and Tsukita, S. (1998). Rho-kinase phosphorylates COOH-terminal threonines of ezrin/radixin/moesin (ERM) proteins and regulates their head-to-tail association. *J. Cell Biol.* **140**, 647-657.
McClatchey, A. I., Saotome, I., Ramesh, V., Gusella, J. F. and Jacks, T. (1997). The Nf2 tumor suppressor gene product is essential for extraembryonic development immediately prior to gastrulation. *Genes Dev.* **11**, 1253-1265.
Morales, F. C., Takahashi, Y., Kreimann, E. L. and Georgescu, M. M. (2004). Ezrin-radixin-moesin (ERM)-binding phosphoprotein 50 organizes ERM proteins at the apical membrane of polarized epithelia. *Proc. Natl. Acad. Sci. USA* **101**, 17705-17710.
Omori, Y. and Malicki, J. (2006). oko meduzy and related crumbs genes are determinants of apical cell features in the vertebrate embryo. *Curr. Biol.* **16**, 945-957.
Radice, G. L., Rayburn, H., Matsunami, H., Knudsen, K. A., Takeichi, M. and Hynes, R. O. (1997). Developmental defects in mouse embryos lacking N-cadherin. *Dev. Biol.* **181**, 64-78.
Shook, D. and Keller, R. (2003). Mechanisms, mechanics and function of epithelial-mesenchymal transitions in early development. *Mech. Dev.* **120**, 1351-1383.
Tam, P. P. and Gad, J. M. (2004). Gastrulation in the mouse embryo. In *Gastrulation: From Cells to Embryo* (ed. C. D. Stern), pp. 233-262. Cold Spring Harbor: Cold Spring Harbor Laboratory Press.
Tepass, U., Theres, C. and Knust, E. (1990). crumbs encodes an EGF-like protein expressed on apical membranes of Drosophila epithelial cells and required for organization of epithelia. *Cell* **61**, 787-799.
Tsukita, S. and Yonemura, S. (1999). Cortical actin organization: lessons from ERM (ezrin/radixin/moesin) proteins. *J. Biol. Chem.* **274**, 34507-34510.
Wei, X. and Malicki, J. (2002). nagie oko, encoding a MAGUK-family protein, is essential for cellular patterning of the retina. *Nat. Genet.* **31**, 150-157.
Wodarz, A., Hinz, U., Engelbert, M. and Knust, E. (1995). Expression of crumbs confers apical character on plasma membrane domains of ectodermal epithelia of Drosophila. *Cell* **82**, 67-76.
Yamada, T., Pfaff, S. L., Edlund, T. and Jessell, T. M. (1993). Control of cell pattern in the neural tube: motor neuron induction by diffusible factors from notochord and floor plate. *Cell* **73**, 673-686.
Zohn, I. E., Li, Y., Skolnik, E. Y., Anderson, K. V., Han, J. and Niswander, L. (2006). p38 and a p38-interacting protein are critical for downregulation of E-cadherin during mouse gastrulation. *Cell* **125**, 957-969.